Supporting Information

Lee et al. 10.1073/pnas.1003572107

SI Text

SI Materials and Methods

Plasmids, strains, and proteins. All constructs were cloned into pPROEX HTb (Invitrogen). The plasmid encoding full-length Hsp104 (pGALSc104b) was a gift from Dr. Susan Lindquist, the Cys-free pseudo wild-type T4L mutant (pHS1403) was a gift from Dr. Brian Matthews and Dr. Zhefeng Guo, and yeast Ydj1 was cloned from pJC25YDJ1 (Addgene). Hsp104 was cloned by PCR from pGALSc104b generating pHsp104. To identify stable subdomains, purified Hsp104 was subjected to limited proteolysis. A tryptic digest of full-length Hsp104 resulted in an 84,275 Da trypsin-resistant fragment that was identified by electron spray ionization mass spectrometric analysis and N-terminal amino acid sequencing to consist of residues 157–908, corresponding to an NTD-truncated Hsp104. Hsp104(157–908) ($Hsp104_{\Delta N}$) was cloned by PCR from pHsp104. The Hsp104 Trap mutant variant (E285A and E687A), pTRAP, was generated from pHsp104 by site-directed mutagenesis using QuikChange (Stratagene) and cassette mutagenesis. $Trap_{\Delta N}$ was cloned by PCR from pTrap.

Trap variants harboring a StrepII-tag were generated by PCR followed by cassette mutagenesis. To do so, a 300–700 base pair fragment upstream of a desired site was cloned by PCR with an *Age*I site. The downstream fragment was PCR amplified with primers bearing a StrepII-tag coding sequence and another *Age*I site. The two PCR fragments were ligated using the *Age*I site and then inserted into pTrap using internal restriction enzyme sites.

$Hsp104_{T4L}$ was cloned by inserting a T4L fragment (residues 2–159) between Asn467 and Glu468 of Hsp104, flanked by a Ser-Gly- and Glu-Phe-linker on the N-terminal and C-terminal insertion site, respectively. Primers were designed to introduce complementary overlapping sequences of 18 bases on the respective ends of three PCR products: 5′ and 3′ part of the *Sac*II/*Sal*I cassette (encoding Thr374 to Asp542) of pHsp104, and the T4L fragment, which were then used in overlap extension PCR. The resulting fragment was swapped with the *Sac*II/*Sal*I cassettes of either pHsp104 or pTrap resulting in $pHsp104_{T4L}$ and $pTrap_{T4L}$, respectively.

Proteins were produced in *Escherichia coli* BL21 (DE3) RIL codon plus cells (Stratagene). Expression was induced with 0.5 mM IPTG for 4 h at 30 °C (Ydj1), 4 h at 25 °C (Hsp104, Trap, $Hsp104_{\Delta N}$, $Trap_{\Delta N}$, and StrepII-tagged Trap variants), or 18 h at 16 °C ($Hsp104_{T4L}$ and $Trap_{T4L}$). Proteins were purified from the soluble lysate on a Ni-NTA agarose column. The poly-His-tag was cleaved off with His_6-tobacco etch virus protease and reapplied to the same column to remove the liberated His-tag, the protease, and any uncleaved His-tagged protein. Proteins were further purified by binding to Toyopearl Butyl-650S (Tosoh) and Q-sepharose Fast Flow (GE Healthcare) for Ydj1, and Q-sepharose Fast Flow for Hsp104 and mutant variants, followed by size-exclusion chromatography on a HiLoad 16/60 Superdex 200 column (GE Healthcare) for the $Hsp104_{T4L}$ chimera.

CryoEM. Hexamers were prepared by incubating Trap (0.4 mg/mL) or $Hsp104_{\Delta N}$ (0.3 mg/mL) at 30 °C for 5 min with either 5 mM ATP (Trap) or 1.5 mM ATPγS ($Hsp104_{\Delta N}$) in buffer consisting of 50 mM MOPS pH 7.5, 2 mM DTT, and 10 mM $MgCl_2$. 3.0 μL of sample was applied to glow discharged copper grids (Quantifoil), blotted, and frozen in liquid ethane essentially as described (1). To image the Hsp104-T4L chimera, purified $Trap_{T4L}$ (0.05 mg/mL) in 50 mM MOPS pH 7.5, 80 mM KCl, 5 mM $MgCl_2$, and 1 mM DTT was incubated with 1 mM ATP for 5 min at 22 °C. Once assembled, $Trap_{T4L}$ hexamers were stabilized by glutaraldehyde crosslinking (0.05% v/v) and imaged by cryoEM.

Multimodel refinement. A multimodel refinement step was included at the beginning to sort particles of different conformations. Multimodel refinement was necessary due to different side views in reference-free 2D class averages. Details of single-model (2, 3) and multimodel refinement (4) have been described. An initial model for the Trap hexamer was generated from reference-free class averages, and refined with 6-fold symmetry applied. This model was low-pass filtered to 40 Å and 10% of random noise was applied to generate two or three different starting models for multimodel refinement. Particles were classified according to their similarity to a set of projection views obtained from each starting model and used to produce new reference models. This process was iterated for 40 cycles until the particle number in each set no longer changed significantly.

Atomic structure fitting of the Trap hexamer. First, the ClpB monomer was fitted as an intact rigid body into the cryoEM map via the AAA-1 domain. The Hsp104 hexamer was generated from the fitted monomer structure by applying a 6-fold rotational symmetry matrix, producing a model that resembles the cryoEM reconstruction in overall shape and dimension. To optimize the fit, the AAA-1 and AAA-2 domains were split, and the AAA-2 ring was rotated by 23° around the 6-fold axis, followed by a 19° rotation around the hinge region connecting the D2-large and D2-small domains. Pairwise comparison shows that the AAA-2 domain in the EM fit is rotated by 19° and translated by 15 Å relative to the crystal structure when superimposed via the AAA-1 domain (Fig. 2*B*). Finally, the NTD was fitted into the cryoEM densities, followed by modeling the linker regions that connect the NTD and AAA-1, and AAA-1 and AAA-2 domains.

Dot blot analysis. StrepII-tagged Trap hexamers were isolated in 25 mM Hepes pH 7.5, 150 mM KOAc, 50 μM ATP, 10 mM $Mg(OAc)_2$, 5% glycerol, and 1 mM DTT on a Superose 6 HR 10/300 column (GE Healthcare) (Fig. S2). Prior to the dot blot assay 5 mM ATP was added to the protein sample to stabilize the Hsp104 hexamer. 0.25 μg and 1 μg of hexamer sample (0.6 mg/mL) was applied to a nitrocellulose membrane and blocked with 3% BSA in Tris-buffered saline and 50 μM ATP. Blots were probed for 1 h at 23 °C with a monoclonal antibody-HRP conjugate (IBA) against the StrepII-tag. Membranes were washed and processed for chemiluminescence (Pierce).

To prepare StrepII-tagged Trap monomers, KCl was added to a final concentration of 300 mM to the purified protein in the absence of ATP. It was previously shown that high salt concentrations destabilize the apo Hsp104 hexamer (5). No nucleotide was added. 0.25 μg and 1 μg of sample was applied to a nitrocellulose membrane and blocked with 3% BSA in Tris-buffered saline but without ATP. Blots were probed for 1 h at 23 °C with the same commercial monoclonal antibody and processed as described above. Notably, Tween-20 was omitted from all Western blotting, because it was previously reported that Tween-20 interferes with Hsp104 hexamerization (6).

Biochemical assays. Enzymes used in assays were purchased from Roche and Hsp104 model substrates from Sigma–Aldrich unless indicated otherwise. All molar concentrations of proteins refer to monomers. Trap variants (6 μM) were incubated for 20 min at 22 °

C in buffer A (25 mM Hepes pH 7.5, 150 mM KOAc, 10 mM $Mg(OAc)_2$, 10 mM DTT) supplemented with 2 mM ATP and 0.2 mg/mL κ-casein. Hexamer samples were analyzed on a Superdex 200 HR 10/30 column (GE Healthcare) in buffer A containing 1 mM ATP.

ATPase activities were measured at 30 °C in buffer A with 2 mM ATP and a coupled ATP regenerating system consisting of 1 μM pyruvate kinase, 1 μM lactate dehydrogenase, 0.5 mM phosphoenolpyruvate, and 0.2 mM NADH. ATP hydrolysis was calculated from the oxidation of NADH, as monitored at 340 nm on a UV-1601 Spectrophotometer (Shimadzu).

For refolding assays, 10 μM firefly luciferase (Promega) was denatured in 8 M Urea in buffer A for 30 min at 22 °C and then diluted 100-fold into buffer A with 1 μM Hsp104, 1 μM human Hsp70 (Stressgen), 1 μM Ydj1, 2 mM ATP, 20 mM phosphoenolpyruvate, and 2 μM pyruvate kinase. Luminescence was measured in 50 mM Tris-glycine pH 7.5 with 0.15 mM luciferin and 2.5 mM ATP using a LS 55 fluorescence spectrometer (PerkinElmer). 0.4 μM *E. coli* β-gal was denatured in buffer A at 60 °C for 40 min, and then diluted in an equivolume of buffer A containing chaperones (final concentrations as above) at 22 °C. β-gal activities were measured as described (7).

1. Lee S, Choi JM, Tsai FTF (2007) Visualizing the ATPase cycle in a protein disaggregating machine: Structural basis for substrate binding by ClpB. *Mol Cell* 25:261–271.
2. Ludtke SJ, Baldwin PR, Chiu W (1999) EMAN: Semiautomated software for high-resolution single-particle reconstructions. *J Struct Biol* 128:82–97.
3. Ludtke SJ, Chen DH, Song JL, Chuang DT, Chiu W (2004) Seeing GroEL at 6 Å resolution by single particle electron cryomicroscopy. *Structure* 12:1129–1136.
4. Chen DH, Song JL, Chuang DT, Chiu W, Ludtke SJ (2006) An expanded conformation of single-ring GroEL–GroES complex encapsulates an 86 kDa substrate. *Structure* 14:1711–1722.
5. Hattendorf DA, Lindquist S (2002) Cooperative kinetics of both Hsp104 ATPase domains and interdomain communication revealed by AAA sensor-1 mutants. *EMBO J* 21:12–21.
6. Wendler P, et al. (2009) Motor mechanism for protein threading through Hsp104. *Mol Cell* 34:81–92.
7. Freeman BC, Morimoto RI (1996) The human cytosolic molecular chaperones hsp90, hsp70 (hsc70), and hdj-1 have distinct roles in recognition of a nonnative protein and protein refolding. *EMBO J* 15:2969–2979.

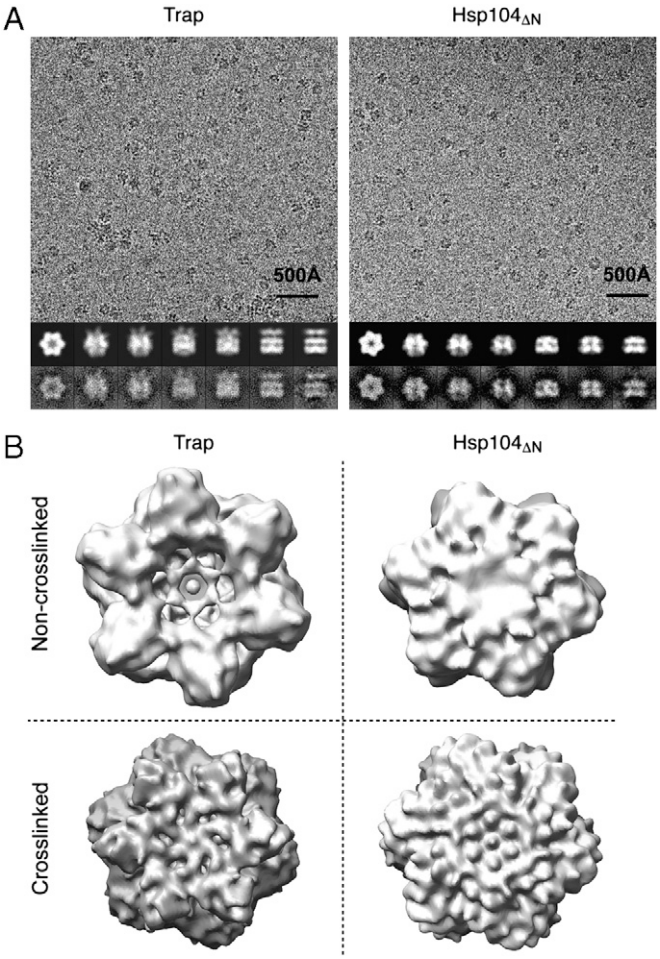

Fig. S1. CryoEM analysis of two Hsp104 variants. (*A*) Representative area of digital micrographs of the noncrosslinked Trap-ATP (*Left*) and $Hsp104_{\Delta N}$-ATPγS hexamer (*Right*). The figure also shows selected projection views (*Top Row*) and corresponding class averages (*Bottom Row*) for each reconstruction. (*B*) Top down views of the isosurface representations of the noncrosslinked (*Upper*) and glutaraldehyde crosslinked (*Lower*) Trap-ATP (*Left*) and $Hsp104_{\Delta N}$-ATPγS hexamer (*Right*).

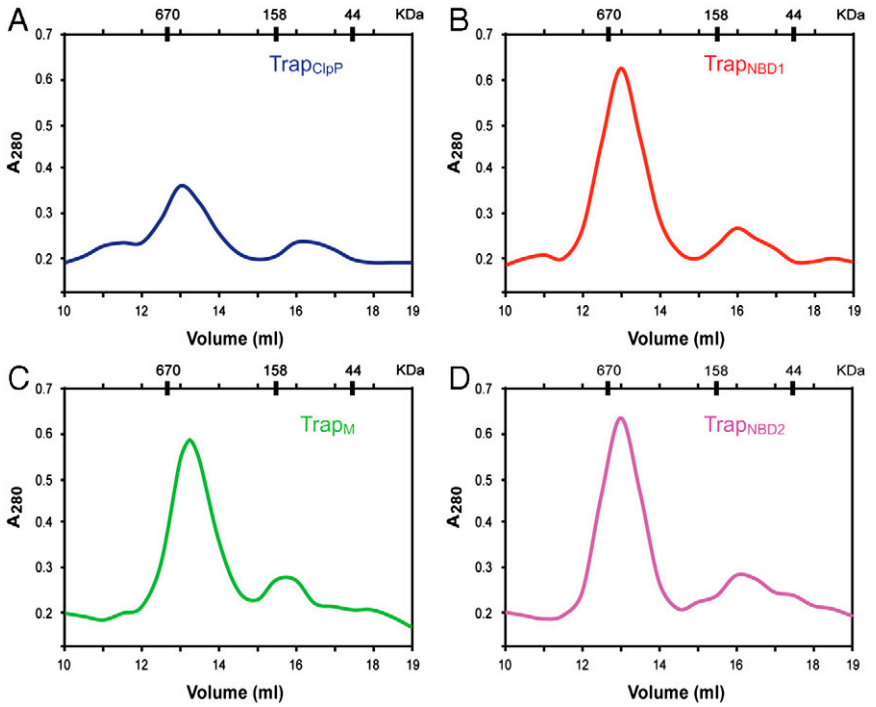

Fig. S2. StrepII-tag containing Trap variants form hexamers in the presence of ATP as determined by size-exclusion chromatography. Hexamer assembly of purified (*A*) Trap$_{ClpP}$, (*B*) Trap$_{NBD1}$, (*C*) Trap$_{M}$, and (*D*) Trap$_{NBD2}$ analyzed by size-exclusion chromatography. Positions of molecular weight standards are indicated.

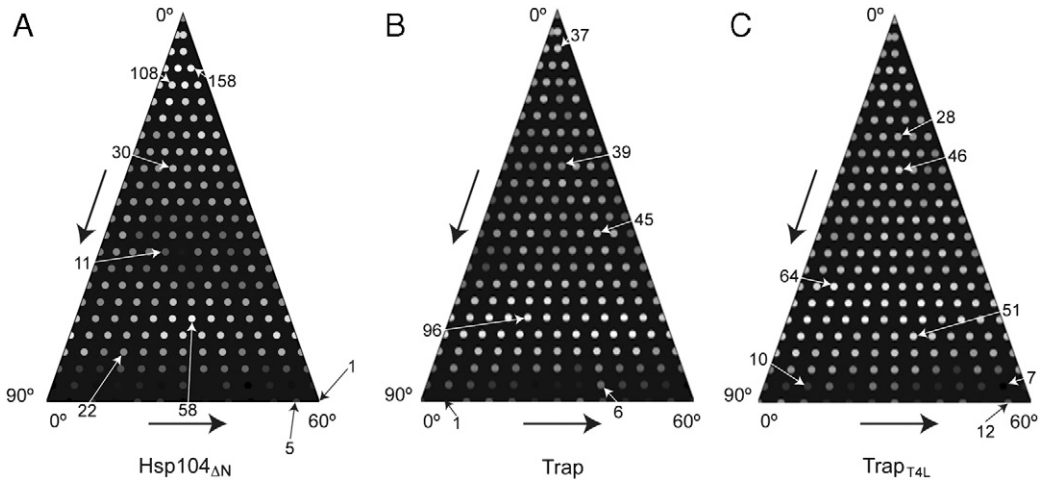

Fig. S3. Distribution of particle orientations over an asymmetric unit used in the cryoEM reconstructions. (*A*) Hsp104$_{\Delta N}$-ATPγ*S*, (*B*) Trap-ATP, and (*C*) Trap$_{T4L}$-ATP. Brighter dots indicate a larger number of particles. For clarity several dots are labeled with the number of particles found.

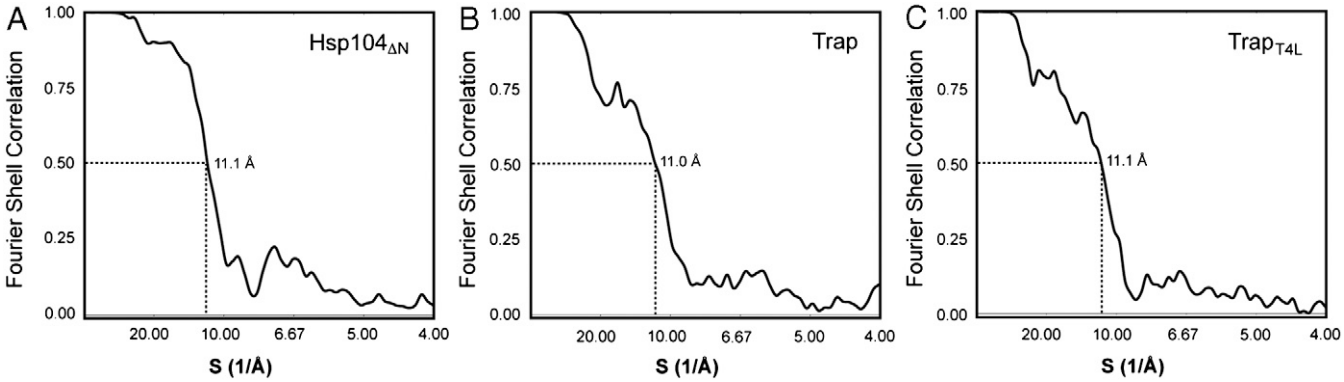

Fig. S4. Fourier shell correlation between reconstructions from even and odd halves of the datasets. A threshold of 0.5 was used to assess the resolution of the final cryoEM reconstructions: (*A*) Hsp104$_{\Delta N}$-ATPγS, (*B*) Trap-ATP, and (*C*) Trap$_{T4L}$-ATP.

Table S1. Summary of the data used for the cryoEM reconstructions

CryoEM reconstruction	Total number of particles included in refinement	Total number of particles used in the final class averages	Final resolution (Å)
Trap-ATP (noncrosslinked)	7,174	5,804	11.0
Hsp104$_{\Delta N}$-ATPγS (noncrosslinked)	7,036	5,647	11.1
Trap-ATP (crosslinked)	15,898	13,944	10.3
Hsp104$_{\Delta N}$-ATPγS (crosslinked)	13,055	10,413	10.1
Trap$_{T4L}$-ATP (crosslinked)	8,689	6,678	11.1